AN ABSTRACT OF THE THESIS OF

Jon Tate Eliason for the Master of Science in Physics

Date thesis is presented: October 8, 1965

Title: TEMPERATURE DEPENDENCE OF INTERNAL FRICTION IN SILICON AT LOW FREQUENCY

Abstract approved: Redacted for Privacy
(Major Professor)

This investigation represents a previously unreported method of measurement of internal friction in single crystals of silicon. The method consists of exciting a rectangular reed of silicon of uniform cross section into forced vibration at its resonant frequency. The end of the reed is silver plated and eddy currents induced in the silver plate by an oscillating magnetic field interact with an inhomogenous permanent magnetic field to provide the periodic driving force. Values of the internal friction Q^{-1}, and the strain amplitude ϵ, are then determined from optical measurements. The entire device is maintained in a vacuum chamber at pressures less than 60 microns of Hg.

The results indicate that the values of Q^{-1} in silicon are below the lower limit of resolution of the apparatus used. However, an upper limit of $Q^{-1} < 3 \times 10^{-4}$ at a frequency of 81 cps and at temperatures from 20°C to 130°C can be placed. These results are compared with projected data of Southgate and Attard.

TEMPERATURE DEPENDENCE OF INTERNAL FRICTION IN SILICON AT LOW FREQUENCY

by

JON TATE ELIASON

A THESIS

submitted to

OREGON STATE UNIVERSITY

in partial fulfillment of
the requirements for the
degree of

MASTER OF SCIENCE

June 1966

APPROVED:

Redacted for Privacy

Professor of Physics

In Charge of Major

Redacted for Privacy

Chairman of Department of Physics

Redacted for Privacy

Dean of Graduate School

Date thesis is presented October 8, 1965

Typed by Audrey McFarlin

ACKNOWLEDGEMENTS

I am very grateful and indebted to Dr. James J. Brady, who throughout the period of time of this investigation has been very encouraging and helpful. My sincere thanks go to Dr. Brady and to Dr. E. A. Yunker of the O.S.U. Physics department for the use of their time and equipment. To Dr. James Looney, of the O.S.U. Electrical Engineering department, I am also indebted for providing me with the silicon used in this experiment and also for the use of his laboratory facilities, both of which were offered graciously. My thanks also go to Tektronics, Inc. and to the U.S. Bureau of Mines for their help in preparing and analyzing the reed material, respectively. To my wife, Barbara, I cannot express my appreciation sufficiently for her patience and help. Last but not least, I am grateful to Mrs. Audrey McFarlin for agreeing to type this thesis.

TABLE OF CONTENTS

	Page
INTRODUCTION	1
APPARATUS	6
PREPARATION OF THE REEDS	12
METHOD OF MEASURING INTERNAL FRICTION	25
RESULTS	28
CONCLUSIONS	33
BIBLIOGRAPHY	40
APPENDIX	42

FIGURES

1.	Diagram of reed, vise, and transducer	9
2.	Diagram of the apparatus	10
3.	Block diagram of electrical circuitry	11
4.	Data exhibiting the jump phenomenon	21
5.	Comparison between thermocouple and thermometer temperatures	35
6.	Variation of internal friction with temperature	36
7.	Variation of internal friction with pressure.	37
8.	Variation of fibration amplitude with pressure	38
9.	Variation of internal friction with strain amplitude ($T = 30^{\circ}C$)	39
10.	Variation of internal friction with strain amplitude ($T = 133^{\circ}C$).	39

TABLES

Page

1. Reed dimension changes in two etches as a function of time 15

2. Data of this investigation 61

3. Sample data sheet 65

TEMPERATURE DEPENDENCE OF INTERNAL FRICTION IN SILICON AT LOW FREQUENCY

INTRODUCTION

Internal friction is a generic name for the irreversible internal processes which result in the mechanical damping of an isolated piece of material. As an example, when a stress is applied to a material, the strain may not all occur simultaneously but may lag the stress. The measures of this effect are called relaxation times and are the times for the strain to increase or decrease to within 1/e (where e is the basis of natural logarithms) of the difference between final value of strain and the strain which occurs simultaneously with the applied stress. Internal friction may also occur in the form of hysteresis in a cyclic mechanical process on the material, requiring that additional energy be supplied during each cycle, i.e., there may be energy losses in the crystal lattice of the material and this energy must be resupplied. This mechanism is analogous to energy loss in a resonant electrical circuit and may be characterized by a value of "Q" or quality of the resonance. Here Q^{-1}, called the "internal friction", is a direct measure of the internal energy lost per cycle in the process. Again, if an isolated material is excited to vibrate, and the driving force is then removed, the material will not vibrate indefinitely but the oscillations will be damped and characterized by some value of logarithmic decrement δ which is related to Q^{-1}. Still a third

manifestation of internal friction is the attenuation of sound waves in a material, characterized by an attenuation coefficient α. The following equalities hold for $\delta << 1$:

$$\delta = \pi Q^{-1} = \frac{1}{2} \frac{\Delta E}{E}$$

where E is the total energy of the vibrating reed and ΔE is the energy loss in one cycle. Also, for pure compression or shear waves

$$\alpha = \frac{\omega}{2c} Q^{-1}$$

where c is the velocity of sound in the material and ω is the angular frequency of the wave (19, p. 352-353).

One method of measuring internal friction consists of using ultrasonic pulse techniques and measuring the attenuation of the sound waves in the material as a function of frequency and amplitude. The frequency range extends through 1 mc/sec to greater frequencies and the method is capable of measuring Q^{-1} as small as 10^{-4} (19, p. 360). In another method, the specimen, usually a rectangular bar, is excited in one or more of its resonant modes and either the decay in amplitude of the vibrations or the Q^{-1} of the resonance measured. Excitation is usually achieved by a transducer. The reported range of frequencies using this method is from approximately 100 cps to 300 kc/sec and values of Q^{-1} as small as to 10^{-7} are attainable. A third method is to measure the logarithmic decrement using optical or electrical techniques and a

torsion pendulum with a fine wire drawn of the material to be studied. This method is suitable for frequencies from 0.1 to 10 cps and to a maximum strain amplitude of about 10^{-5}. A variation of this method uses forced transverse vibrations of a reed and has a frequency range from ten to several thousand cycles per second. The internal friction Q^{-1} is measured rather than the logarithmic decrement. This is the method used in this research.

There are many known mechanisms of internal friction, probably the motion of dislocations have the greatest significance. However, a variety of other mechanisms have large effects and have also been studied extensively. Among these are the motion of impurity atoms between interstitial positions in the crystal lattice, the flow of heat as the result of inhomogeneous deformation of the material (thermoelastic effect), internal phase transitions, grain boundary motion, and motion of the Bloch walls separating magnetic domains in ferromagnetic materials. Because these mechanisms require energy and are irreversible they contribute to internal friction. While these and others are known to be mechanisms of internal friction, the problems of isolating and identifying them in specific situations are great. The task is complicated by the anisotropic nature of crystal lattices, the difficulties of controlling impurities and lattice imperfections, the sensitivity of dislocation density to the history of the material and

the all inclusive macroscopic nature of the measurement. Since it is impossible to eliminate all of the unwanted variables or even to minimize all of them, the only experimental control available is to hold the unwanted conditions as constant as possible while varying, hopefully, only the desired parameters. In spite of these difficulties, the study of internal friction is able to give us information about the Peierl's force which opposes the glide motion of dislocations and general aspects of the interaction between impurity atoms and dislocations.

Silicon was the material chosen for this particular study, because dislocations play an important part in the behavior of silicon as a semiconductor. Electrons and holes tend to gather along dislocation lines, and because dislocations may act as recombination centers, they provide a sink for minority carriers. Because of the distortions in the lattice near dislocations, impurities gather preferentially along them. Also, dislocations act as scattering centers, thereby reducing the mobility of the carriers. Still another effect arises as vacancies created near dislocations act as acceptors, decreasing the electron concentration. For these and other reasons, knowledge of the behavior of dislocations in semiconducting material seems prerequisite to the adequate control of the electrical properties.

It is believed the method chosen for this investigation is its first application to the study of internal friction in silicon. Internal friction in silicon has been studied at much higher frequencies than used in this experiment over the past ten years, but primarily by measuring the attenuation of ultrasonic pulses (9, p. 803) and by measuring the logarithmic decrement of vibrations induced in a rectangular prism suspended at nodal points (17, 18). The method used in this study involves the use of a thin rectangular reed made of single crystal silicon oriented with its longer dimension along the $< \bar{1}11 >$ direction. One end of the reed is clamped in a massive vise while the other end is excited into transverse vibrations with a transducer. The frequency of the driving force is then swept (varied) past the natural resonant frequency of the reed and the value of Q^{-1} determined from optical measurements of the half-power points and a knowledge of the frequency of the driving force. This method will be described in greater detail in a later section.

APPARATUS

Basically, the apparatus consists of a transducer and its associated electronic equipment. The transducer, which provides the driving force for the reed, contains two electromagnets symmetrically positioned about the rest position of the reed. These electromagnets produce an alternating magnetic field which induces eddy currents at the reed tip. The eddy currents interact with an inhomogeneous magnetic field supplied by two permanent magnets above and below the reed to produce the alternating driving force. The relative positions of the magnets and reed are shown in Figure 1. The transducer is excited by a radio frequency oscillator whose output frequency is divided by two banks of binary scalers to obtain a desirable transducer frequency. Frequency reductions in powers of two up to 2^{16} are possible. The output of the scalers is then put through a filtering circuit to remove the higher harmonics, and amplified before reaching the transducer.

The transducer is mounted on and insulated from a rigid frame which also supports the reed vise and the oven. The oven consists of a cylindrical brass tube wrapped on the outside with resistance wires as the heating element. Gaskets made from soft solder were used to vacuum seal the end pieces of the cylinder. Soft solder placed an

upper limit on the temperature of the oven since it was also used extensively with seals for the wires to the transducer. A small window placed in one end of the oven allowed observation of the end of the reed through the microscope (See Figure 2).

The output of the scalers is also used to drive a stroboscope through a phantastron phase shifting circuit. This device allows the position of the tip of the reed to be observed at any portion of the cycle. The maximum vibrational amplitude and half power amplitude are then optically measured with a microscope equipped with a filar eyepiece.

The apparatus used in this investigation was that designed by Jewell (12) and subsequently modified by O-Halloran (15), Larson (13), Falk (7), Coleman (5), and Pradhan (16). It is essentially the same as that used by Pradhan with the exception that two copper-constantan thermocouples were inserted through the oven wall to positions near the sample. In addition, the power supply for the phantastron and univibrator circuits was replaced with a commercial regulated power supply. The thermocouples provided much improved accuracy in measurement of the temperature of the sample and the regulated power supply improved the stability of the stroboscope. A detailed description of the equipment may be found in the theses of the above authors. A

block diagram of the apparatus is shown in Figure 3.

Falk (7), Anderson (2) and Coleman (5) have reported that for several positions of the frequency meter dial, the output frequency at the transducer did not agree with the frequency as calculated from the dial setting and considering the reduction by the scalers. This was checked by observing on an oscilloscope the transducer input voltage frequency as a function of oscillator dial setting. The output of the first scaler was found to have the same frequency as the input accounting for a factor of two previously reported. The outputs of the first two scalers appeared badly distorted. A jump reduction in frequency of the output by a factor of 2/3 was periodically observed, as was reported by Falk (7) at a frequency of approximately 120 cycles per second output and approximately 4,700 on the oscillator dial. Observations of harmonics from the oscillator as high as the twelfth order cause suspicion that these jumps in frequency were due to the response of the scalers to the lower order (2^{nd} and 3^{rd}) harmonics of the frequency meter.

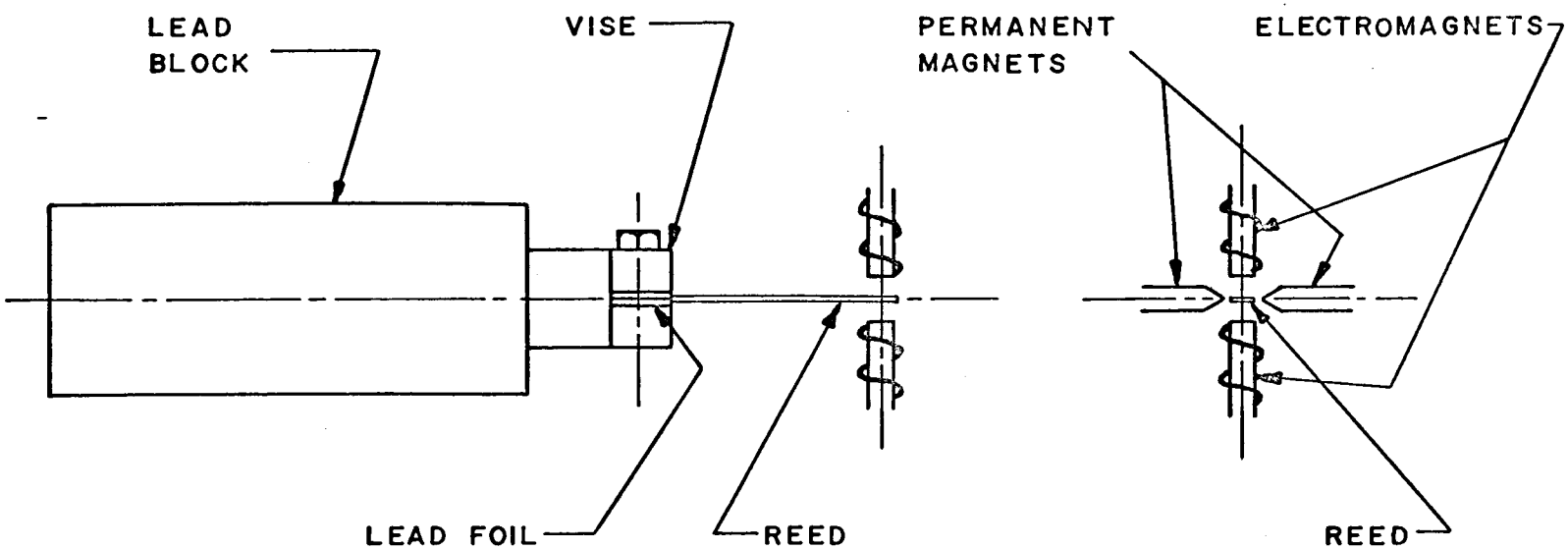

FIGURE I
DIAGRAM OF REED, VISE, AND TRANSDUCER

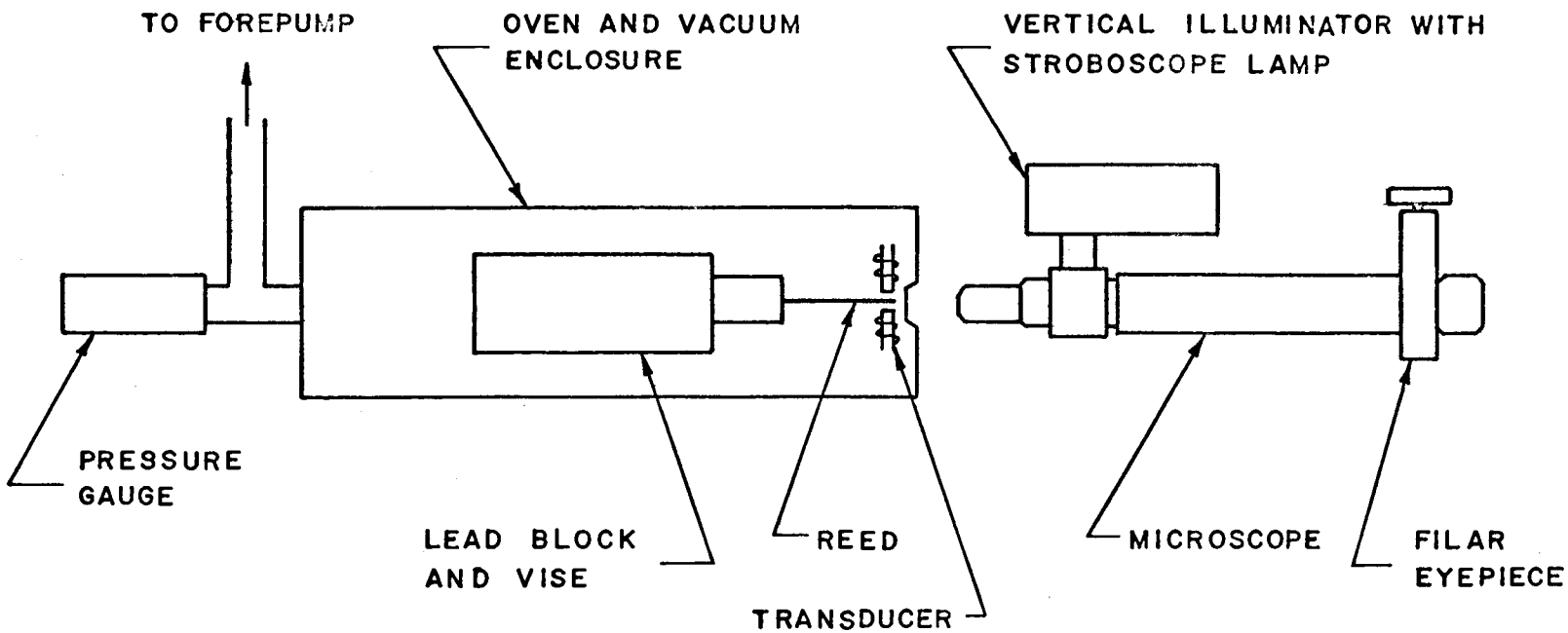

FIGURE 2
DIAGRAM OF THE APPARATUS

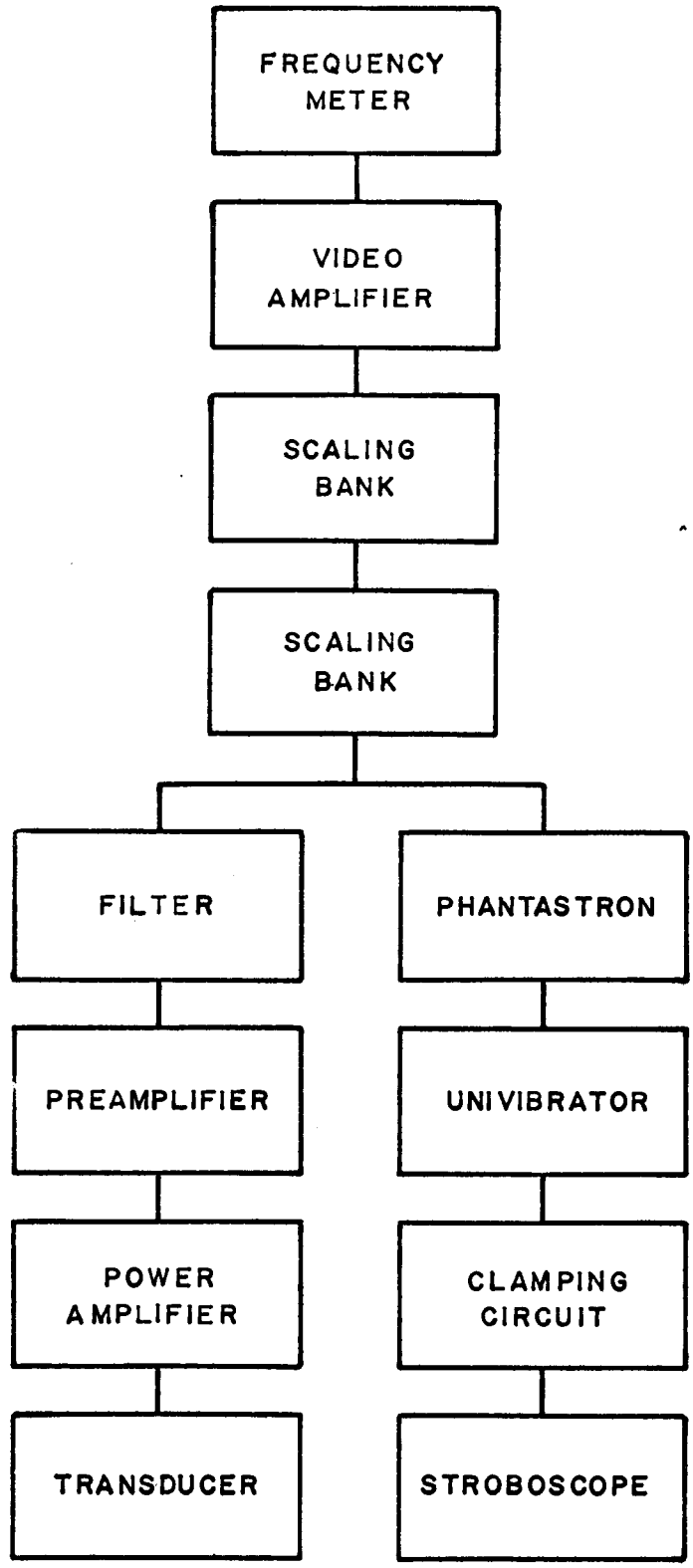

FIGURE 3
BLOCK DIAGRAM OF ELECTRICAL CIRCUITRY

PREPARATION OF THE REEDS

Two parallel slabs of silicon were cut axially from a cylindrical single crystal ingot graciously supplied by Dr. James C. Looney of the Electrical Engineering Department at O.S.U. The ingot was grown with the <111> direction parallel to the axis. Because the diamond saw in Dr. Looney's laboratory was too small, these cuts were made by special arrangement at Tektronix, Inc., in Portland, Oregon. The ingot was first cut on a diameter into two halves. From each of these halves a slice approximately 1/16 inch thick was cut. One slab was accidentally fractured at approximately 2/3 of its length during the cutting but the other remained whole. The slabs of silicon were therefore from adjacent and parallel cuts of the same ingot. These slabs were then roughly lapped to remove the gross saw cuts on their faces and waxed securely to glass lantern slide covers to be cut to the rough size of the reeds. The broken slab was cut into three reeds of approximate size 2-3/8 x 7/64 x 1/32 inches. These reeds were placed in containers labeled 1, 2, and 3. The undamaged slab was later cut into four reeds, three of which were approximately 3 x 1/4 x 1/32 inches and the fourth 3 x 3/16 x 1/32 inches. These reeds were placed in containers labeled 4, 5, 6, and 7 (for the 3/16 inch wide reed), respectively.

A sample of one of the slabs of silicon was analyzed spectroscopically at the U. S. Bureau of Mines in Albany, Oregon. The analysis revealed the following impurities in the silicon:

Ag	3 ppm
Al	30 ppm
Mg	5 ppm
Cu	2 ppm
Ga	30 ppm

A resistivity measurement using the four probe technique indicated a resistivity of 4.0 ohm-cm and a cold probe* test showed the material to be p-type in agreement with the analysis.

Reeds #2 and #3 were waxed to a lantern slide cover plate and simultaneously lapped with #500, #750, #1000, and #2600 corundum abrasive, successively. The reeds were then removed and rewaxed for polishing of the opposite sides. This procedure was used to keep the reeds as identical as possible and also to attempt to grind the faces

---

*If a sample of semiconductor at a uniform temperature is touched by two probes, one at the same temperature as the sample and one at a temperature substantially colder, the localized temperature of the sample near the cold probe is reduced. Because the carrier density in the semiconductor decreases with decreasing temperature, a concentration gradient is created in the neutral material and carriers diffuse from the warmer region into the colder region until the concentration driving force is exactly opposed by the forces on the carriers due an internal electric field. Under open circuit conditions, this electric field may be detected with a potentiometer placed between the two probes. If the majority carriers are holes, i.e., the material is p-type, the cold probe will be positive in potential with respect to the ambient temperature probe.

of the reeds as flat and parallel as possible. This lapping procedure left the reeds with a shiny metallic finish and removed all saw marks. The edges of the reeds were also carefully lapped. Reed #1 was prepared initially by a similar procedure to test the method for subsequent reeds.

Reed #1 was then used to conduct some preliminary tests. Since it was desired to etch the reeds to remove all traces of surface defects, the rate of mass removal from the reeds must not be too rapid because the reeds were thin. Reed #1 was immersed in two common acid etchants, acid etchant b (10 parts HNO_3 to 1 part HF) and CP-5 (5 parts HNO_3 to 3 parts HF to 3 parts acetic acid)(11, p. 6-16), to determine their dimension change rates. The reed was successively immersed in the etchant, rinsed in distilled water after each immersion and thickness and width measured. The results are indicated in Table 1. The results are quite erratic since an oxide layer appears to form rapidly on the silicon when it is removed from the etch. This film is resistant to the etch and the reaction is very slow until this film is removed, after which the reaction is rapid and the etchant bubbles vigorously. Both etchants appeared to lose strength quite rapidly, both with use and with age. It was noted that defects such as scratches and chips seemed to be attacked preferentially and other

TABLE 1

REED DIMENSION CHANGES IN TWO ETCHES
AS A FUNCTION OF TIME

Etchant type	Time in etch (sec.)	Width (10^{-3} inches)	Thickness (10^{-3} inches)
Acid etchant b*	0	221.0	29.5
	15	220.5	29.3
	30	220.5	29.3
	90	220.5	29.2
	180	219.5	29.0
	480	218.0	28.4
	780	218.0	28.0
	1080	216.5	27.6
CP-5**	0	216.0	27.8
	15	215.5	27.0
	30	215.0	26.2
	45	214.0	25.3
	60	213.5	25.3
	90	213.0	24.5
	180	208.0	22.1
	220	207.0	21.1

* 10 parts HNO_3, 1 part HF

** 5 parts HNO_3, 3 parts HF, 3 parts acetic acid. A third etchant was tried, containing 4 parts HNO_3, 4 parts HF, 1 part H_2SO_4, but this was found to react much too rapidly to be useful.

areas attacked hardly at all. It was resolved to do a better job of cleaning the silicon before etching in the future to remove all oil and other contaminants. Plastic gloves were hence forth used in handling the reeds, and before etching each reed was individually and carefully washed in separate vessels containing water, carbon tetrachloride and methanol, successively, to remove all traces of wax, oil, and abrasive. This procedure subsequently resulted in a highly polished and relatively scratch-free surface on the silicon.

Reed #1 was again lapped with #1000 corundum and re-etched in CP-5 and 30 seconds. The dimensions before and after etching are given below.

Reed #1	Before	After
Thickness:	0.0133 inches	0.0116 inches
Width:	0.2075	0.2058
Length:	2.34	2.34

This read was inserted into the vise of the apparatus to a free length of 1.75 inches. The resonant frequency of the reed is given by (14, p. 112)

$$\omega_n = (k_n L)^2 \left[\frac{a}{2\sqrt{3}}\right]\left[\frac{1}{L^2}\right]\left[\frac{E}{\rho}\right]^{1/2}$$

where a is the reed thickness, b the breadth, L the length, ρ the mass density, and E the modulus of elasticity. The first resonant frequency occurs for $k_n L \approx 1.875$. Preliminary claculations showed that the reed

would be expected to vibrate at a frequency of 203 cycles per second but that it would require one thousand times the power or more* to induce vibrations with amplitude similar to that of metal reeds tested by previous experimenters. Fruitless searching for a resonance proved this estimate to be reasonably correct. Several methods to increase the oscillatory force at the end of the reed eventually succeeded. These included increasing the permanent magnetic field by moving the magnets closer together, operating with maximum gain in the power amplifier and painting the tip of the reed with a light coat of electrically conducting paint. In this process, the vise end of the reed was broken and the effective cantilever length was reduced to 1.56 inches. Under these conditions the reed was observed to resonate with small amplitude at a frequency of 156 cycles per second.

---

*For small values of Q^{-1}, most of the power supplied to the reed is assumed to be dissipated thermally by the induced currents circulating at the tip of the reed. For two reeds of identical dimensions then,

$$\frac{P_1}{P_2} = \frac{I_1^2 \rho_1}{I_2^2 \rho_2}$$

where P is the power supplied, I is the induced current, and ρ is the resistivity of the reed. Since the force on the reed depends on the value of the induced current, for comparable deflections of the tip of the reed we must set $I_1 = I_2$. For a metal reed $\rho \approx 10^{-4}$ ohm-cm while for this sample of silicon $\rho = 4.0$ ohm-cm. Therefore approximately 4×10^4 more power must be supplied to the silicon reed than the metal reed for a comparable deflection.

After this initial trial series of tests, several problems were evident. One, the vise jaws had to be reworked to remove irregularities which would create high stresses in the brittle silicon. This was accomplished by lapping the two jaws together with abrasive, creating two surfaces that matched as perfectly as possible and were quite flat. This precaution all but eliminated one cause of reed breakage. Another but more important problem was that of increasing the amplitude of vibration of the reed, which was still too small to obtain data over the range of amplitude desired. Success in this effort was finally obtained by plating a highly conducting metal onto the tip of the reed. Copper plating was tried and found unsuccessful. Satisfactory results were finally obtained by depositing silver on the surface of the silicon using the Rochelle Salts Process (4, p. 2997) followed by plating with silver from a silver nitrate solution. Since the silver and silicon do not form a silicide and the eutectic temperature of the silver-silicon system is 830^{o}C (10, p. 51), no significant interaction between the two materials is expected at the temperatures of this experiment.

Reeds #2 and #3 were etched for approximately 50 seconds in CP-5 and silver plated at the tips as described above. Reed #1 was not useful with its painted tip after plating was successful. The dimensions of

reeds #2 and #3 before and after etching are given below.

Reed #2	Before	After
Length:	2.08 inches	2.08 inches
Width:	0.2630	0.2596
Thickness at end 1:	0.0096	0.0081
Thickness at center:	0.0083	0.0069
Thickness at end 2:	0.0104	0.0089
Reed #3	**Before**	**After**
Length:	2.36 inches	2.36 inches
Width:	0.2646	0.2619
Thickness at end 1:	0.0106	0.0090
Thickness at center:	0.0112	0.0099
Thickness at end 2:	0.0096	0.0084

Minor equipment problems became the next order of importance. The stroboscope light was barely bright enough to see the end of the reed and flashed irregularly. Part of the trouble proved to be an old lamp, and part a poor connection in the socket. The major trouble proved to be low power supply voltage to the phantastron phase shifting circuit which triggered the stroboscope. Reworking the circuit back to the original schematic solved this problem. Reoccurring dimness of the lamp after prolonged operation was thought to be due to the thermally caused degradation of the electrical contacts of the lamp with the socket. Another minor but confusing problem concerned the constant shifting of the reference point readings of the rest position of the reed. Several days were spent trying to attribute this shifting to thermal effects, loose bolts, nonrigid supports, internal stresses, etc., when it was finally decided that the culprit was the microscope itself. A small

amount of looseness in the focusing mechanism resulted in substantial movement of the magnified image. Reworking the mechanism in the machine shop helped, but satisfactory operation was obtained only with the help of rubber bands to hold the barrel of the microscope firmly to one side.

The equipment was finally in satisfactory operating condition to begin to obtain data. Several reproducibility tests were run in air and were satisfactory using reed #2. The system was then sealed in the oven and operated at room temperature and at a pressure of approximately 40 microns of Hg. Four runs were attempted at different power levels with erratic results. The maximum amplitude of the reed appeared to change and the measurement of the half power frequencies was not consistent. Examination of the apparatus revealed no apparent cause. A detailed point by point measurement of vibration amplitude versus frequency revealed the strikingly assymmetric resonance curve shown in Figure 4. When the frequency of vibration was being increased the discontinuity in the curve was found to occur at a different frequency than when the frequency of vibration was being decreased. Reed #2 was then removed from the vise and reed #3 was inserted to a free length of 1.75 inches. Again a discontinuous resonance curve was observed. The apparatus was again examined for faulty operation and the frequency meter output checked for discontinuous operation. The

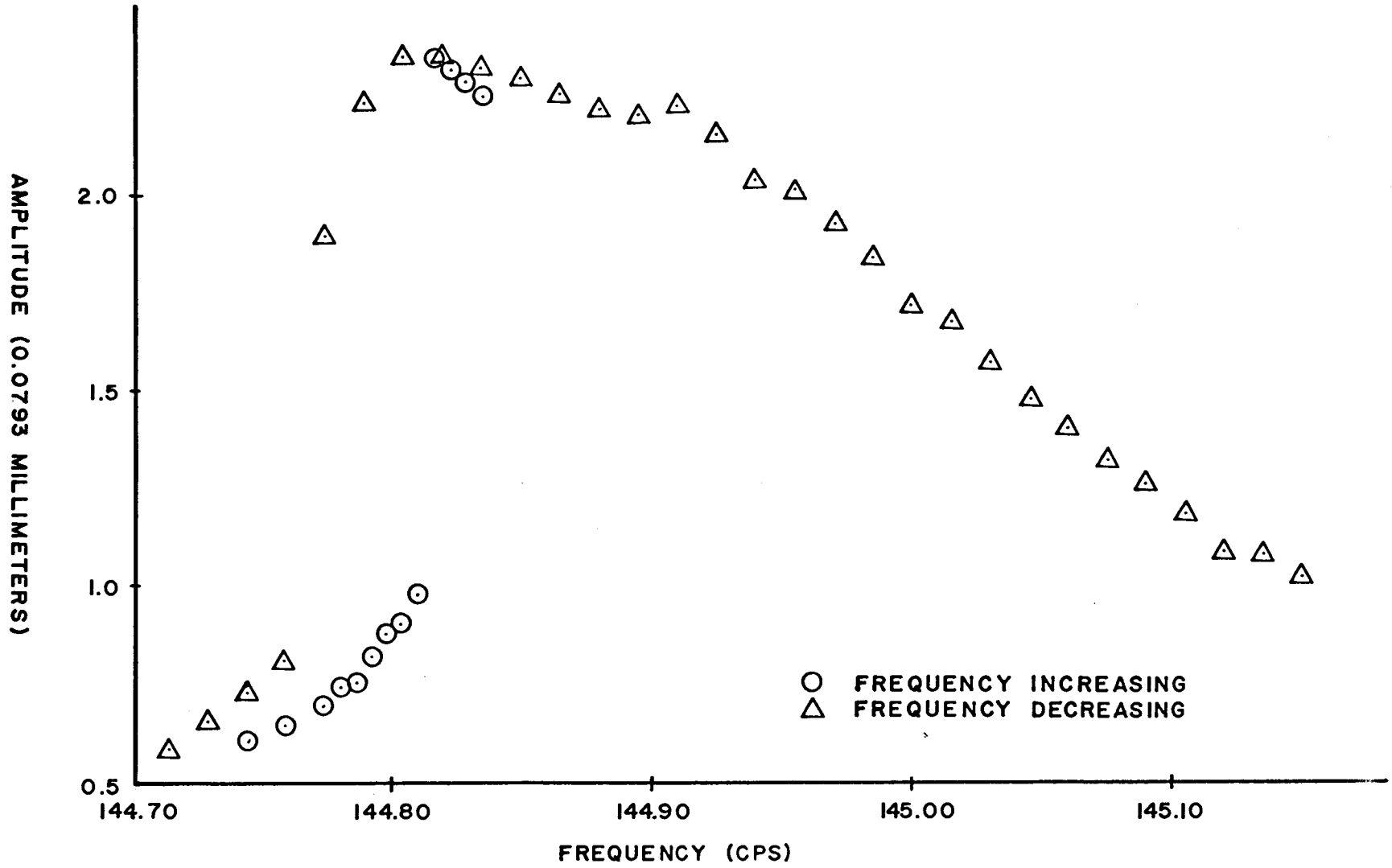

FIGURE 4
DATA EXHIBITING THE JUMP PHENOMENON

power supplied, power amplifier, and phase shifting circuits all appeared to operate perfectly in the range used. In a further attempt to improve stable operation, an unregulated power supply for the pre-amplifier in the transducer driving circuitry was replaced with an Oregon Electronics Variable Voltage Regulated Power Supply, to reduce any possible power line effects. Using great care in conducting another run, including maintaining constant voltages, an invariable reference point, reliable phase control of the stroboscope, and extreme care not to bump the equipment especially the microscope, the experiment was repeated with essentially the same results, i.e., another discontinuous resonance curve. Noteworthy was the fact that the exact point of the discontinuity was not reproducible and appeared to represent an unstable condition of the reed. Operation of the reed at amplitudes between the points of discontinuity was not possible, and once the jump occurred, either toward greater or lesser amplitude, the amplitude of the vibration would increase or decrease its full measure. This change did not occur instantaneously but over a period of several seconds. A thin metal reed used by previous experimenters (unknown composition) was tested in the same manner but with the result that the resonance curve was symmetrical and did not exhibit the discontinuous effect.

At this unfortunate time both reeds #2 and #3 were broken in handling.

Reeds #4, #5, #6, and #7 were prepared for use. Dimensions before and after a 30 to 60 second etching are listed below. Reed #5 was broken during washing and reed #7 chipped in handling.

Reed #4	Before	After
Length:	3.00 inches	3.00 inches
Width:	0.2443	0.2375
Thickness at end 1:	0.0107	0.0091
Thickness at center:	0.0108	0.0089
Thickness at end 2:	0.0116	0.0098
Mass before plating:	0.2395 gm	
Mass after plating:	0.2430 gm	

Reed #5	Before	After
Length:	1.89 inches	1.89 inches
Width:	0.2355	0.2343
Thickness at end 1:	0.0098	0.0095
Thickness at center:	0.0101	0.0093
Thickness at end 2:	0.0099	0.0092
Mass	0.1510 gm	

Reed #6	Before	After
Length:	3.00 inches	3.00 inches
Width:	0.2360	0.2340
Thickness at end 1:	0.0122	0.0109
Thickness at center:	0.0115	0.0105
Thickness at end 2:	0.0122	0.0112
Mass	0.2780 gm	

Reed #7	Before	After
Length:	3.00 inches	3.00 inches
Width:	0.1899	0.1856
Thickness at end 1:	0.0140	0.0139
Thickness at center:	0.0138	0.0127
Thickness at end 2:	0.0152	0.0130
Mass	0.2695 gm	

All essential parameters of the experiment had been tested and checked except the method of clamping the reed in the vise. Two sheets of lead 1/16 inch thick were inserted between the brass jaws of the vise and reed #4 inserted with a free length of 2-3/8 inches. The resonant amplitude versus frequency behavior was then observed at different power levels. No discontinuity in the vibration amplitude was observed, and there was no striking asymmetry as evident in the previous data. The lead evidently provided an intimate contact with the reed instead of a partial contact between two hard surfaces. This resulted in the removal of nonlinear effects of the partial contact, returning the system to that of the linearly damped system. McLachlan (14, p. 56-62) and other books on vibrations treat this subject. All subsequent testing was performed with the lead foil in the vise. According to Hansen (10, p. 1106), lead and silicon do not alloy, and do not form solid solutions. At temperatures above 1000°C, however, liquid lead dissolves a small amount of silicon (0.15 at atomic % at 1250°C). No interaction should thus be expected between lead and silicon at the temperatures of this experiment.

METHOD OF MEASURING INTERNAL FRICTION

The details of the procedure for the measurement of data points are given below. Initially, the vise was removed from the apparatus and the reed carefully inserted, positioned with respect to scratches on the vise and clamped between the lead jaws. The free length of the reed was measured. Some adjustment of the position was necessary to ensure proper location of the reed between the magnets and this was accomplished by means of adjustable screws on the vise and on the frame of the apparatus. Vacuum seals were made from solder in the shape of an "O" ring and the oven was sealed and evacuated. When the chamber reached operating pressure and the associated electronic equipment had been warmed up for at least an hour, the following observations were made.

With no power to the transducer and the reed stationary at its rest position, the end of the reed was observed through the microscope and some reference point such as a scratch or bright spot was chosen. The hair line in the filar eyepiece was then aligned on the image of this reference point and the reading used as the rest position of the reed. A sixteen millimeter objective was used on the microscope so that one hundred units of the eyepiece scale corresponded to a 0.0793 mm displacement of the end of the reed.

A standard data sheet was made and reproduced to ease the task of recording the data. A sample of the data sheet is included in the appendix. At the beginning and end of each run the time, pressure, and temperature were recorded. The run number, transducer voltage, reed identification, frequency reduction factor, and other pertinent experimental conditions were noted for each run. The frequency of the frequency meter and the stroboscope light phase relative to the vibrating reed were then varied simultaneously until the maximum amplitude of the reed was found. The frequency meter dial reading and the filar eyepiece setting were then recorded and the procedure repeated twice more and average values obtained. The reed frequency corresponding to this average dial reading was then recorded. Subtracting the rest position reading on the eyepiece scale from the average reading obtained for the maximum displacement gives the resonant amplitude of the reed. Since power is proportional to the square of the amplitude, the half-power amplitude is obtained by taking 0.707 of the resonant amplitude. The filar eyepiece was adjusted to this reading and the oscillator frequency and stroboscope phase delay varied until this amplitude of vibration was obtained. This procedure was employed twice, once for the upper half-power point and once for the lower half-power point. The corresponding meter frequency for each of these points was recorded on the data sheet. The difference in the reed half-power frequencies divided

by the frequency at resonance then yields the internal friction Q^{-1}.

The maximum longitudinal strain amplitude ϵ is given by the ratio of the resonant amplitude y times the reed thickness t to the square of the length L of the reed which is free to vibrate.

$$\epsilon = ty/L^2$$

Multiplying the resonant amplitude expressed in units as measured with the filar eyepiece by 0.793×10^{-1}, gives the amplitude "y" in millimeters.

RESULTS

Data were obtained for transducer voltages of 1.0 to 4.0 volts rms and over the temperature rante 20°C to 130°C. Reed #4 was used exclusively in obtaining the final data. Runs #1 through #9 were preliminary tests. Final measurements were made in runs #10 through #42 beginning at room temperature and proceeding to maximum temperature. The oven and reed were then slowly cooled down and the reed and vise were removed from the oven and examined. Again, reed #4 was re-inserted in the vise and installed in the oven. The oven was evacuated and the same procedure used to take data for runs #43 through #75 over a similar temperature range. This second series of runs was performed with modifications in the vacuum system and method of measuring temperature. The path length from the evacuated system to the fore pump was reduced and pressures of 30 μ Hg were attained at the high temperature conditions as opposed to 60 μ Hg on the first series of runs. Two copper-constantan thermocouples were inserted through the oven wall into the region near the reed, one into the vise and the other into the open space near the reed. On the second series of runs these thermocouple temperatures were compared with the thermometer readings. Thermocouple potentials were measured with a Leeds and Northrup Company Volt Potentiometer type 8687, O.S.U. inventory number 98615, and were referred to cold junctions in an ice-water bath

and calibrated before use. A comparison of the measured thermocouple temperature with the measured thermometer temperatures is presented in Figure 5 based on these runs.

The results of this investigation are presented in Figures 6 through 10. The data from which these results are derived are tabulated in Table 2 in the appendix. Figure 6 shows the measured values of Q^{-1} as a function of 1/T for the two series of runs with reed #4. Figure 7 shows the same results plotted as a function of the pressure in the oven. The accuracy of the measurement of Q^{-1} is limited by the accuracy to which the half-power frequencies may be measured. The dial of the frequency meter is equipped with a vernier scale enabling one to position the dial to within 0.1 division. The effect of backlash in the mechanism was not estimated but every effort was made to take readings by movement of the dial in one direction only. In the range of operation of the frequency meter in this experiment, including the reduction in frequency of 2^{11}, the apparatus was capable of creating in the reed known frequency changes of 1.38×10^{-3} cycle per second. This number equates to a minimum resolution of Q^{-1} of 1.7×10^{-5}. However, at any given value of Q^{-1}, the accuracy to which that value of Q^{-1} is known is $\pm 3.4 \times 10^{-5}$. This precision is an underestimate if care is not taken in eliminating the effects of the frequency meter tuning control backlash. The solid lines shown in Figure 7

represent this error band. It is clear from examination of this figure that gas pressure significantly affects the measured value of internal friction and that temperature effects, if any, are masked. Figure 8 shows a marked dependence of amplitude of vibration on gas pressure. Error bands of $\pm$ 10% are shown to indicate the approximate range of values for which the apparatus was capable of maintaining the reed driving force constant. The voltage input to the transducer is the indicated parameter.

Figures 9 and 10 show measured values of Q^{-1} as a function of strain amplitude at room temperature and at maximum operating temperature, respectively. Within the accuracy of the data, it is seen that Q^{-1} is a constant function of strain amplitude over the range of temperatures of this experiment.

According to the Granato and Lücke theory of damping due to dislocations (8), a frequency dependent loss and a strain-amplitude dependent, frequency independent loss are possible. The frequency dependent loss is the hysteresis type loss which occurs when the dislocations in a high stress field break away from impurity pinning points during rising stress, only to collapse as the stress relaxes. Clearly, since the data of this investigation is amplitude independent,

we are not concerned with the latter type loss. The former type loss should be relatively temperature independent up to some temperature limit, since the internal friction is proportional to the dislocation loop length and this is fixed primarily by the density of impurity pinning points until the temperature is great enough to cause significant numbers of breakaway loops. When this temperature is reached, the internal friction should become temperature dependent and proportional to $\exp(-H/kT)$ where H is an activation energy for breakaway (See, for example, discussions in references 8, 9).

Amplitude and temperature independent contributions to Q^{-1} may also arise from the thermoelastic effect and losses to the apparatus. The thermoelastic contribution to internal friction has been well described by Zener in two papers (20, 21). The maximum contribution of the macroscopic thermoelastic effect has been calculated in the appendix to occur at a frequency of 2,410 cycles per second. Its contribution at the frequency of this experiment is negligible. A calculation of effective internal friction due to apparatus losses, also given in the appendix, shows the value of Q^{-1} from this source may be as much as 8.6×10^{-5}. That the presence of gas, even at a pressure of 30 μ Hg contributes significantly to Q^{-1} is apparent from the data. Calculations assuming a Boltzmann velocity distribution for air in the chamber near

the reed indicate that the contribution to Q^{-1} at a pressure of 30 μ Hg is 1.6×10^{-4}. These calculations are included in the appendix. Attempts to further reduce the pressure in the oven or the losses to the apparatus would mean extensive apparatus design changes.

At 3.0 kilocycles per second and at a temperature of 1000°K, Southgate and Attard (18) have measured the logarithmic decrement of single crystals of silicon to be 1.70×10^{-4}. This value corresponds to $Q^{-1} = 5.34 \times 10^{-5}$. Even at 600 Kelvin degrees higher temperature this value is an order of magnitude smaller than the values determined in this experiment. The exhibited frequency dependence of the data of Southgate and Attard does not offset the temperature dependence when these data are extrapolated to 81 cycles per second and 130°C.

CONCLUSIONS

This investigation resulted in the determination of values of internal friction varying from (2.5 to 3.5) x 10^{-4} over the temperature range 20°C to 130°C using a single crystal silicon reed. These measurements were made with the reed vibrating at a frequency of 81 cycles per second. The curves of internal friction versus strain amplitude are characterized by amplitude independence and there appears to be a definite correlation of both internal friction and strain amplitude with the pressure of gas in the oven.

While there is some basis in the dislocation theory of internal friction to expect a frequency dependent, temperature independent behavior over a range of temperatures up to some maximum value, a comparison with the data obtained by Southgate and Attard seems to indicate that the expected values of internal friction would be substantially less than those found in this investigation. Similarly, the contributions of the thermoelastic effect to internal friction at 81 cycles per second are negligible compared with the measured values. A calculation of the effect of energy losses to the supporting structure of the reed, indicates that this loss mechanism may contribute an effective value of internal friction of 8.6 x 10^{-5}. However, calculations substantiated by the data indicate the major contribution is due to the presence of gas in the oven. At a pressure of 30 μ Hg at 300°K,

this contribution was calculated to be 1.6×10^{-4}. It is therefore concluded that the true value of internal friction is less than 3×10^{-4}, i.e., it is below the available resolution of the apparatus used in this experiment.

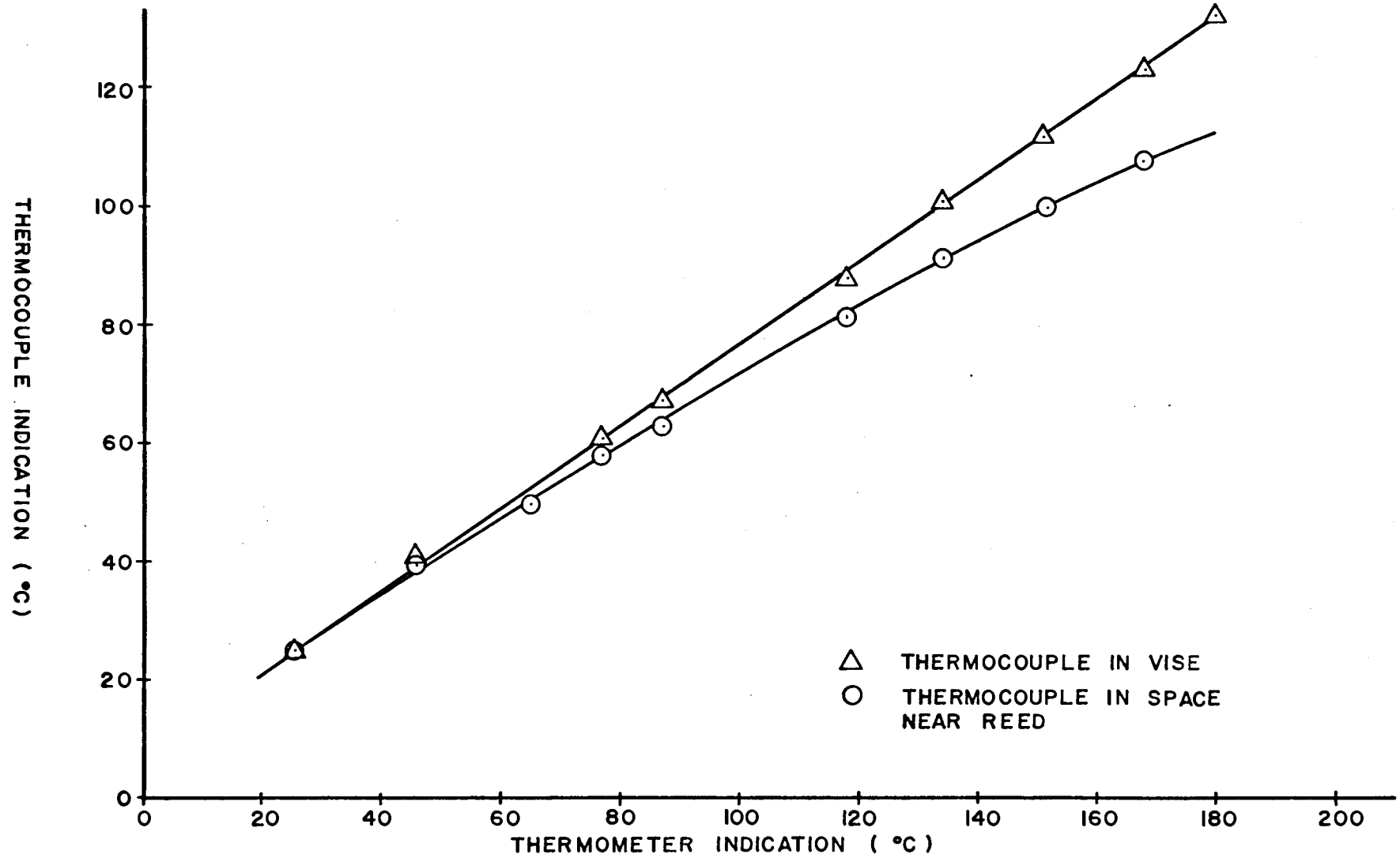

FIGURE 5
THERMOCOUPLE - THERMOMETER COMPARISON

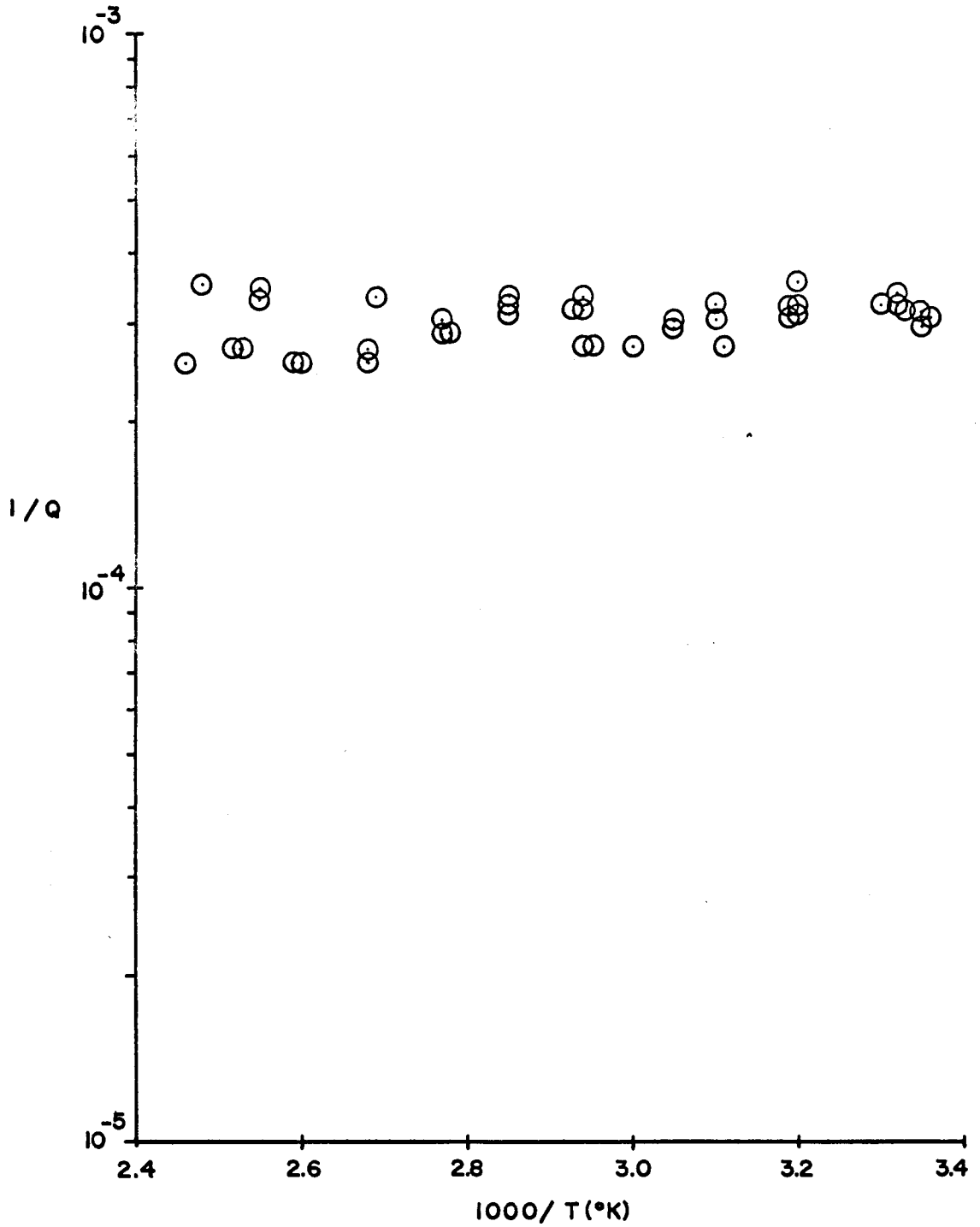

FIGURE 6
VARIATION OF INTERNAL FRICTION
WITH TEMPERATURE

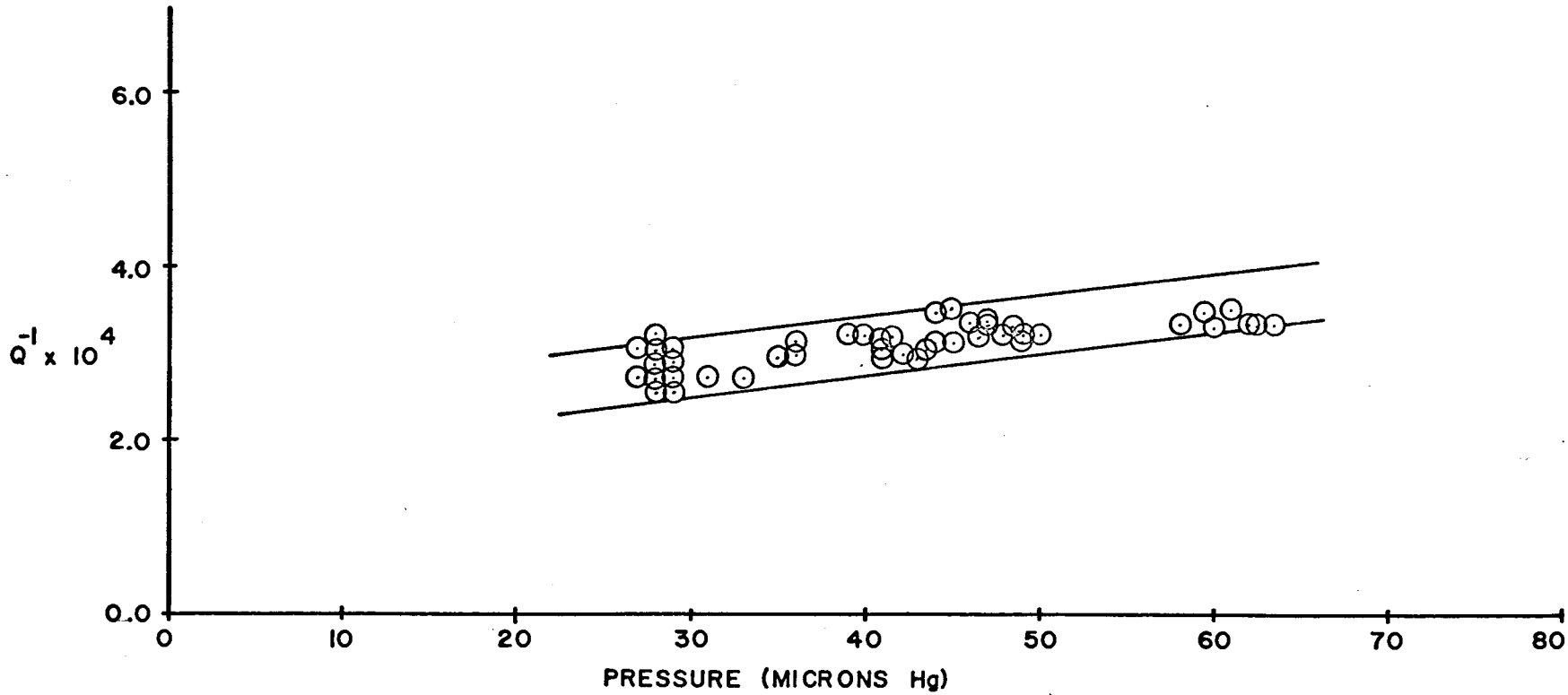

FIGURE 7

VARIATION OF INTERNAL FRICTION

WITH PRESSURE

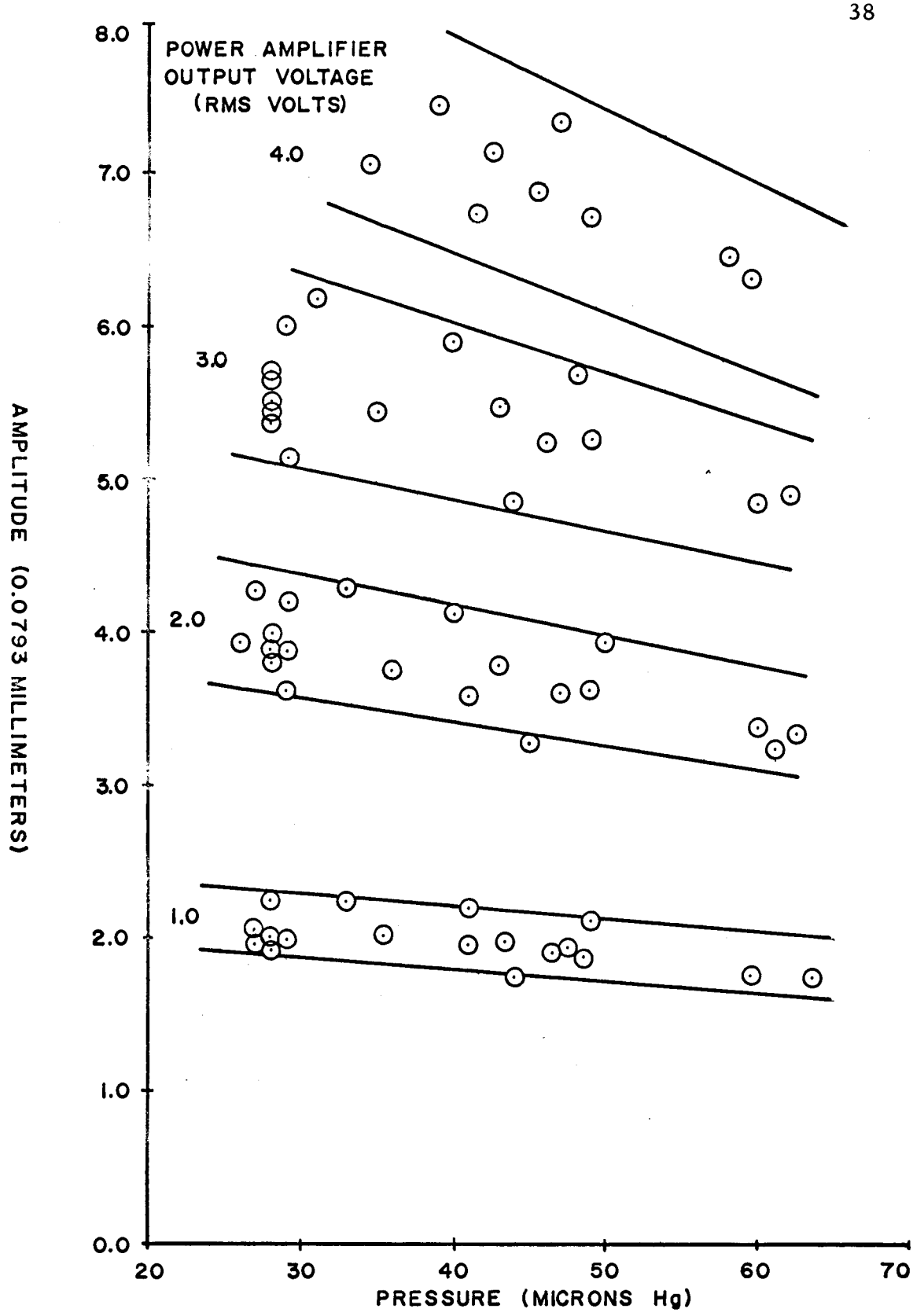

FIGURE 8
VARIATION OF VIBRATION AMPLITUDE
WITH PRESSURE

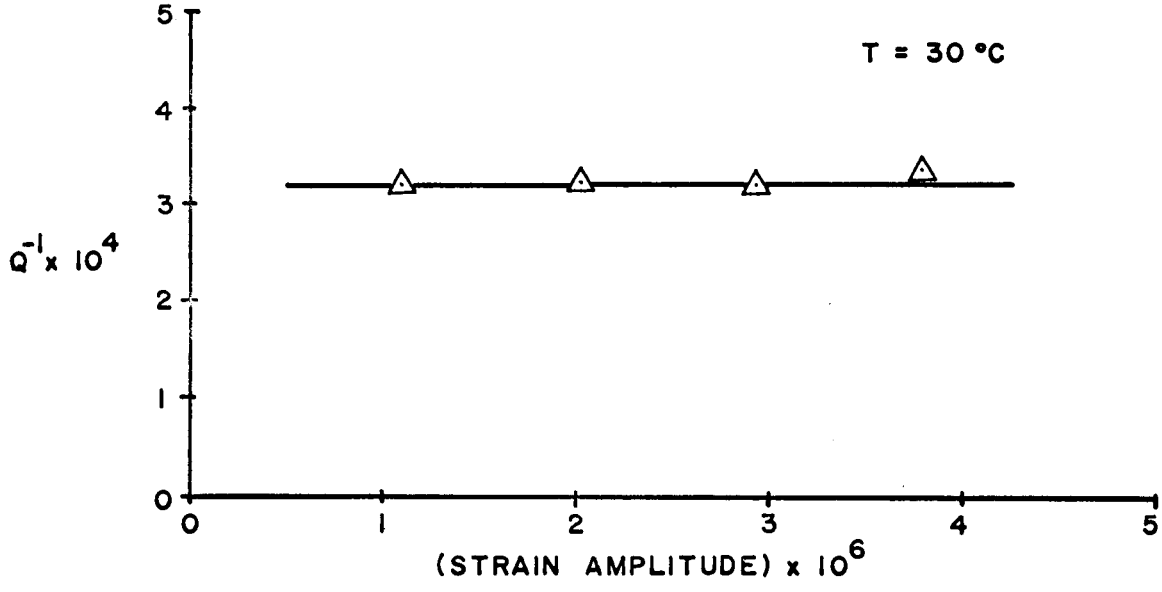

FIGURE 9
VARIATION OF INTERNAL FRICTION
WITH STRAIN AMPLITUDE

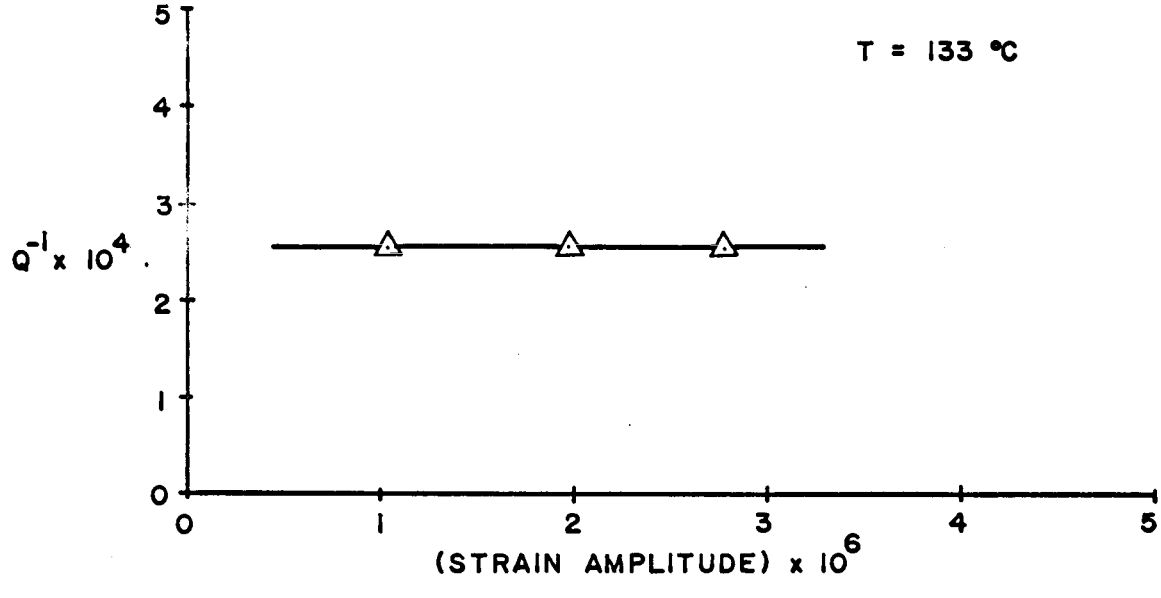

FIGURE 10
VARIATION OF INTERNAL FRICTION
WITH STRAIN AMPLITUDE

BIBLIOGRAPHY

1. American Institute of Physics. American Institute of Physics handbook. 2d ed. New York, McGraw-Hill, 1963. 1 vol.

2. Anderson, Merlin F. The effect of cold-working upon the internal friction of annealed polycrystalline copper. Master's thesis. Corvallis, Oregon State College, 1956. 47 numb. leaves.

3. Brailsford, A. D. Abrupt-kink model of dislocation motion. Physical Review 122:778-786. 1961.

4. Chemical Rubber Co. Handbook of chemistry and physics. 36th ed. Cleveland, 1954. 3173 p.

5. Coleman, Lamar W. Internal friction of zirconium as a function of annealing conditions. Master's thesis. Corvallis, Oregon State College, 1957. 58 numb. leaves.

6. Cottrell, A. H. Dislocations and plastic flow in crystals. London, Oxford University Press, 1963. 223 p.

7. Falk, E. D. The effect of annealing temperature upon internal friction for polycrystalline copper. Master's thesis. Corvallis, Oregon State College, 1956. 54 numb. leaves.

8. Granato, A. and K. Lücke. Theory of mechanical damping due to dislocations. Journal of Applied Physics 27:583-593. 1956.

9. _____. Application of dislocation theory to internal friction phenomena at high frequencies. Journal of Applied Physics 27:789-805. 1956.

10. Hansen, M. Constitution of binary alloys. New York, McGraw-Hill, 1958. 1305 p.

11. Hunter, Lloyd P. (ed.) Handbook of semiconductor electronics. 2d ed. New York, McGraw-Hill, 1962. 1 vol.

12. Jewell, William R. A technique for measuring internal friction in vibrating reeds. Master's thesis. Corvallis, Oregon State College, 1948. 109 numb. leaves.

13. Larsen, Milton B. Effect of vibration frequency on the internal friction of cold-worked copper. Master's thesis. Corvallis, Oregon State College, 1955. 43 numb. leaves.

14. McLachlan, N. W. Theory of vibrations. New York, Dover Publications, 1951. 154 p.

15. O'Halloran, T. A. Changes in the internal friction in copper after cold working. Master's thesis. Corvallis, Oregon State College, 1955. 43 numb. leaves.

16. Pradhan, Shaker P. Activation energies for impurities in vanadium from measurements of internal friction. Ph. D. thesis. Corvallis, Oregon State University, 1962. 96 numb. leaves.

17. Southgate, P. D. Internal friction in germanian and silicon. Proceedings of the Physical Society 76:385-408. 1960.

18. Southgate, P. D. and A. E. Attard. Thermally activated dislocation kink motions in silicon. Journal of Applied Physics 34:855-863. 1963.

19. Van Bueren, H. G. Imperfections in crystals. Amsterdam, Netherlands, North Holland Publishing Co., 1961. 676 p.

20. Zener, Clarence. Internal friction in solids. I. Physical Review 52:230-235. 1937.

21. _____. Internal friction in solids. II. Physical Review 53:90-101. 1938.

APPENDIX

CALCULATIONS OF THE FREQUENCY AT WHICH MACROSCOPIC THERMAL CURRENTS CONTRIBUTE THEIR MAXIMUM EFFECTS TO INTERNAL FRICTION

The frequency, f_o, at which macroscopic thermal currents contribute their maximum effects for a reed of rectangular cross section vibrating transversely, is given by (20, p. 233):

$$f_o = \frac{\pi}{2} \frac{D}{t^2}$$

where D = thermal diffusivity = $\frac{k}{\rho c_p}$

t = thickness of the reed = .0093 inches = .0236 cm

For silicon at 20°C:

ρ = density = 2.32 $\frac{gm}{cm^3}$

k = thermal conductivity = 1.50 $\frac{watts}{cm\,K^o}$

c_p = specific heat = .181 $\frac{calories}{gm\,K^o}$

$$D = \frac{1.50}{2.32 \times .181 \times 4.185} = .854 \frac{cm^2}{sec}$$

$$f_o = \frac{3.14 \times .854}{2 \times (.0236)^2} = 2410 \text{ cycles per second}$$

CALCULATION OF THE CONTRIBUTION OF THE THERMOELASTIC EFFECT TO INTERNAL FRICTION AT THE CONDITIONS OF THIS EXPERIMENT

The value of internal friction due to the thermoelastic effect is given by (21):

Eq. 1 $$Q^{-1} = \frac{E_s - E_r}{E_s} \frac{f_o f}{f_o^2 + f^2}$$

where E_s = adiabatic modulus of elasticity

E_t = isothermal modulus of elasticity

f = resonance frequency of vibration corresponding to Q^{-1}

f_o = resonance frequency of vibration corresponding to the maximum value of Q^{-1}

This is shown by Zener (21, p. 93) to reduce to:

Eq. 2 $$Q^{-1} = \frac{TE_t \alpha 2}{C_p} \frac{f_o f}{f_o^2 f^2}$$

where T = temperature in ^oK

α = linear thermal expansion coefficient

C_p = specific heat per unit volume at constant pressure

$C_p = c_p \rho$

ρ = density

c_p = specific heat at constant pressure

For silicon at 300°K, f = 81 cps, f_o = 2410 cps

$$E_t = 16.57 \times 10^{11} \frac{\text{dynes}}{\text{cm}^2}$$

$$c_p = .181 \frac{\text{calories}}{\text{gm K}^\circ}$$

$$\rho = 2.32 \frac{\text{gm}}{\text{cm}^3}$$

$$\alpha = 2.5 \times 10^{-6} \frac{1}{\text{K}^\circ}$$

Substituting these values into Eq. 2,

$$Q^{-1} = (1.77 \times 10^{-4}) \frac{f_o f}{f_o^2 + f^2}$$

for f = 81 cps

$$Q^{-1} = 5.88 \times 10^{-6}$$

CALCULATION OF THE EFFECT OF APPARATUS LOSSES ON THE MEASUREMENT OF INTERNAL FRICTION

Consider the simplified problem of the reed mounted in its vise as illustrated in Figure A-1. Assume that all of the energy transferred from the reed to the vise is lost in the supporting structure. Then, if the mass of the reed m, is very much smaller than the mass of the vise and the lead block M, we may assume the angular deflection of the vise θ, to be small and we may treat the reed as a cantilever in a solid stationary wall. The problem then separates into two systems for consideration, as shown in Figure A-2.

The following relationships then hold:

Eq. 1 $$\theta = \frac{y_1}{a}$$

Eq. 2 $$\Gamma = F_1 a = I\ddot{\theta} = \frac{I}{a}\ddot{y}_1$$

Eq. 3 $$F_2 - ky_2 = \frac{m}{2}\ddot{y}_2$$

where I = moment of inertia of block and vise

θ = angular deflection of the vise

Γ = torque applied by reed to vise

k = spring constant of the reed

m = mass of the reed

$F_2 = \mathrm{Re}\, F_o e^{i\omega t}$ = driving force on reed

Letting $y_2 = \mathrm{Re}\, Ae^{i\omega t}$ and substituting in equation 3, we find

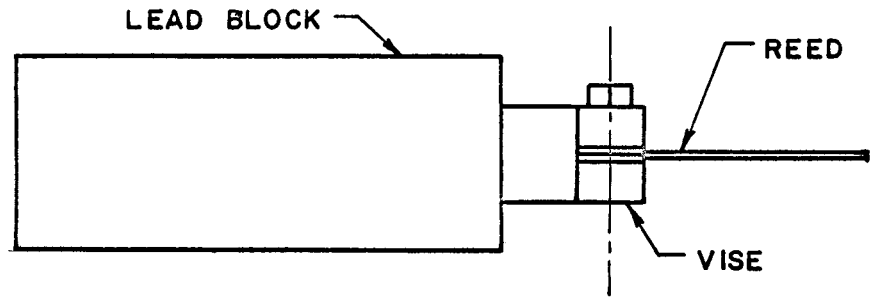

FIGURE A - 1

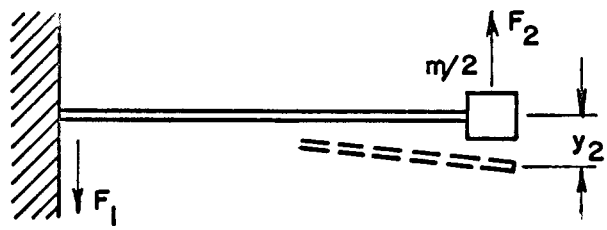

m = MASS OF REED

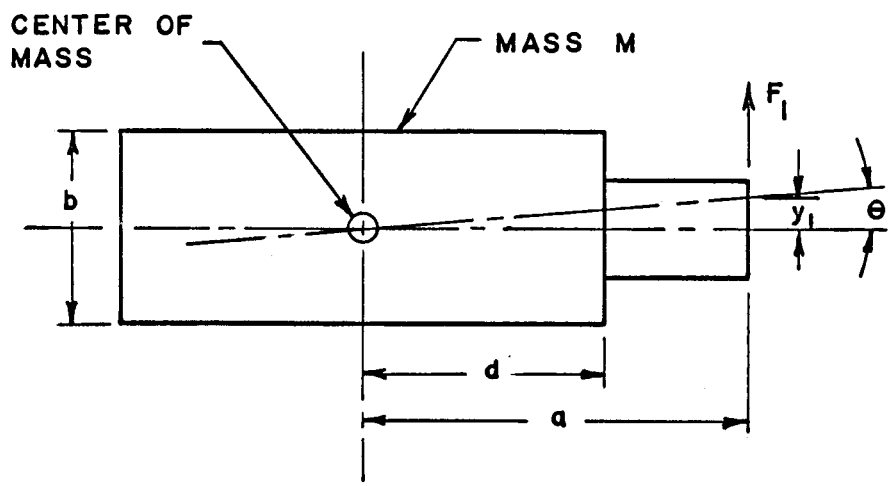

FIGURE A-2

$$A = \frac{F_o}{\frac{m}{2}\left(\frac{2k}{m} - \omega^2\right)}$$

Applying Newton's second law to the reed

Eq. 4 $$F_2 - F_1 = \frac{m}{2}\ddot{y}_2$$

from which follows

Eq. 5 $$F_1 = \frac{F_o\left(\frac{2k}{m}\right)}{\left(\frac{2k}{m} - \omega^2\right)} \cos \omega t$$

Using equations 5 and 2,

$$\ddot{y}_1 = \frac{a^2}{I} F_1 = F_o\left(\frac{2ka^2}{mI}\right)\frac{\cos \omega t}{\left(\frac{2k}{m} - \omega^2\right)}$$

which upon integrating and choosing suitable boundry conditions gives

Eq. 6 $$\dot{y}_1 = F_o\left(\frac{2ka^2}{mI}\right)\frac{\sin \omega t}{\omega\left(\frac{2k}{m} - \omega^2\right)}$$

We assume that all the energy ΔE transferred to the lead block by the reed is lost. Since this energy is being continuously transferred from the reed to the block, we take

Eq. 7 $$\Delta E = 4\int_o^{\tau/4} \Gamma\frac{d\theta}{dt}\, dt = 4\int_o^{\tau/4} F_1 \dot{y}_1\, dt$$

where we have used eq. 1.

$$\tau = \frac{2\pi}{\omega} = \text{period of oscillation of the applied force.}$$

Substituting from equation 5 and 6 into equation 7 and integrating gives the energy transferred from the reed to the block in one cycle.

Eq. 8 $$\Delta E = \frac{8 F_o^2 k^2 a^2}{(\frac{2k}{m} - \omega)^2 m \omega^2 I}$$

The energy stored in the reed is equal to the kinetic energy of the reed at $y_2 = 0$.

Eq. 9 $$E = 1/2(\frac{m}{2})(\dot{y}_2)^2_{max}$$

Substituting $(\dot{y}_2)_{max} = \frac{\omega^2 F_o^2}{\frac{m}{2}(\frac{2k}{m} - \omega^2)^2}$

Eq. 10 $$E = \frac{\omega^2 F_o^2}{m(\frac{2k}{m} - \omega^2)^2}$$

The value of the internal friction is shown by Zener (20, p. 232) to be

Eq. 11 $$Q^{-1} = \frac{\delta}{\pi} = \frac{\Delta E}{2\pi E}$$

where δ is the logarithmic decrement. Substituting for E and ΔE from equations 10 and 8, respectively, gives

Eq. 12 $$Q^{-1} = \frac{4k^2 a^2}{m \omega^4 I}$$

While both E and ΔE become infinite at the resonant frequency because no damping was included in the equation of motion of the reed (eq. 3), the ratio $\frac{\Delta E}{E}$ remains finite and well behaved. At resonance

$$\omega = (\frac{2k}{m})^{1/2}$$

Therefore,

Eq. 13 $$Q^{-1} = \frac{a^2 m}{\pi I}$$

The moment of inertia I of the lead block is defined as

$$I_{zz} = \int (r^2 - z^2)\, dm$$

where the z-axis is the axis of rotation of the block,

$$I_{zz} = \rho L \int_{\frac{-b}{2}}^{b/2} \int_{-d}^{d} (x^2 + y^2)\, dx\, dy$$

Eq. 14 $$I_{zz} = \frac{\rho L}{12}\left[8d^3 b + 2d b^3\right]$$

The mass of the block M of thickness L is given by

Eq. 15 $$M = \rho(2d)\, b\, L$$

$$\rho L = \frac{M}{2 d b}$$

Therefore,

Eq. 16 $$I_{zz} = \frac{M}{12}\left[4d^2 + b^2\right] = I$$

Finally, using equations 13 and 16

$$Q^{-1} = \frac{a^2 m}{\pi \frac{M}{12}\left[4d^2 + b^2\right]}$$

Eq. 17 $$Q^{-1} = \left(\frac{3}{\pi}\right)\left(\frac{m}{M}\right)\frac{\left(\frac{a}{d}\right)^2}{\left[1 + \left(\frac{b}{2d}\right)^2\right]}$$

For the conditions of this experiment

$a \approx 4.0$ inches

$b \approx 2.0$ inches

$d \approx 2.5$ inches

$M \approx 6,000$ gm

$m \approx 0.20$ gm

$$Q^{-1} = \left(\frac{3}{\pi}\right)\left(\frac{.20}{6000}\right)\frac{\left(\frac{4}{2.5}\right)^2}{\left[1 + \left(\frac{1}{2.5}\right)^2\right]}$$

$$Q^{-1} = 7.0 \times 10^{-5}$$

When the mass m of the reed is more accurately described as varying along the length of the reed, it is found that a factor of 1.23 is necessary to correct the above simplified approach. Therefore,

$$Q^{-1} = (1.23)(7.0) \times 10^{-5} = \underline{8.6 \times 10^{-5}}$$

The equation of motion of the reed is more exactly described by the equation (14, p. 115)

$$\frac{\partial^2}{\partial x^2}\left(E_r I_r \frac{\partial^2 \xi}{\partial x^2}\right) + m' \frac{\partial^2 \xi}{\partial t^2} = 0$$

with the boundry conditions $\xi = 0,\ x = 0;\ \frac{d\xi}{dx} = 0,\ x = 0;\ \frac{d^2\xi}{dx^2} = 0,\ x = L$

and $\frac{d^3\xi}{dx^3} = \frac{F_o e^{i\omega t}}{E_r I_r}$ at $x = L$. The solution for the displacement at point x and at time t is

$$\xi(x, t) = \left\{\frac{K}{2(1 + Cc)}\right\}\left\{S + s)(\cosh kx - \cos kx)\right.$$

$$\left. - (C + c)(\sinh kx - \sin kx)\right\}$$

where $K = \dfrac{F_o e^{i\omega t}}{k^3 E_r I_r}$, k is defined by the resonance condition

$k^4 = \dfrac{\omega^2 m'}{E_r I_r}$,

$C = \cosh kL$

$c = \cos kL$

$S = \sinh kL$

$s = \sin kL$

$m' = \dfrac{dm}{dx}$

Following a procedure similar to that used previously,

$$F_1 = F_2 - \int_0^L m' \ddot{y}_2 \, dx = F_2 - \int_0^L m' \ddot{\xi}(x) \, dx$$

$$F_1 = F_o \cos \omega t + m' \omega^2 \, \mathrm{Re} \left\{\int_0^L \xi \, dx\right\}$$

$$\ddot{y}_1 = \frac{a^2}{I_{vise}} F_1$$

and $\Delta E = 4 \int_0^{t/4} F_1 \dot{y}_1 \, dt$

after integrating $\ddot{y}_1$ to get $\dot{y}_1$ and substituting, we obtain the energy lost by the reed in one cycle

$$\Delta E = \frac{2a^2 F_o^2}{I_{vise} \omega^2 (1 + Cc)^2} \overline{F_2}$$

where

$$\overline{F_2} = \left\{\frac{2k^4 E_r I_r (1 + Cc) + m'\omega^2\left[(S^2 - s^2) - (C + c)^2 + 2(C + c)\right]}{2k^4 E_r I_r}\right\}^2$$

The energy stored in the reed is

$$E = (1/2)\int_0^L m'(\dot{y}_2)^2 dx$$

$$E = \frac{m'}{2}\int_0^L (\dot{\xi})^2 dx$$

Performing this integration, we find

$$E = \frac{\omega^2 F_o m'(S + s)^2}{8k^7 E_r^2 I_r^2 (1 + Cc)^2}\,\overline{F_1}$$

where

$$F_1 = \left\{\left[1 + \left(\frac{C + c}{S + s}\right)^2\right]\left[(1/4)\sinh 2kL - sC\right]\right.$$

$$+ \left[1 - \left(\frac{C + c}{S + s}\right)^2\right]\left[(1/4)\sin 2kL - cS\right] + kL$$

$$\left. - \left(\frac{C + c}{S + s}\right)(S - s)^2\right\}$$

Again

$$\delta = \frac{\Delta E}{2E} = \frac{8a^2 k^7 E_r^2 I_r^2}{I_{vise}\omega^4 m'(S + s)^2}\,\frac{\overline{F_2}}{\overline{F_1}}$$

Now at resonance

$$k^4 = \frac{\omega^2 m'}{E_r I_r}$$

$kL = 1.875$ for the first resonance (fundamental) and we

have at resonance $(1 + Cc) \rightarrow 0$

$$\overline{F_2} \rightarrow \frac{1}{4}\left[(S^2 - s^2) - (C + c)^2 + 2(C + c)\right]^2$$

Therefore, at resonance

$$Q^{-1} = \frac{a^2 m}{\pi I_{vise}} \left\{ \frac{2\left[(S - s) + 2\left(\frac{C + c}{S + s}\right) - \left(\frac{C + c}{S + s}\right)^2\right]^2}{(1.875)\ \overline{F_1}} \right\}$$

$$Q^{-1} = (1.23) \frac{a^2 m}{\pi I_{vise}}$$

CALCULATION OF THE CONTRIBUTION TO THE VALUE OF INTERNAL FRICTION DUE TO THE PRESENCE OF GAS NEAR THE REED

Assume the reed lies in the y-z plane when at rest, so that the displacement of the tip of the reed is only in the x-direction. For small amplitudes of vibration, we may assume that the surface dS of a small portion of the reed is parallel to the y-z plane. Call $\vec{c}'$ the velocity of dS in the x-direction and u, v, and w the x, y, and z components of velocity $\vec{c}$ of molecules of gas near dS. Let m be the mass of the gas molecules and M the mass of the element of the reed dS. Also, assume the average number of molecules at $\vec{r}$ within $d\vec{r}$,

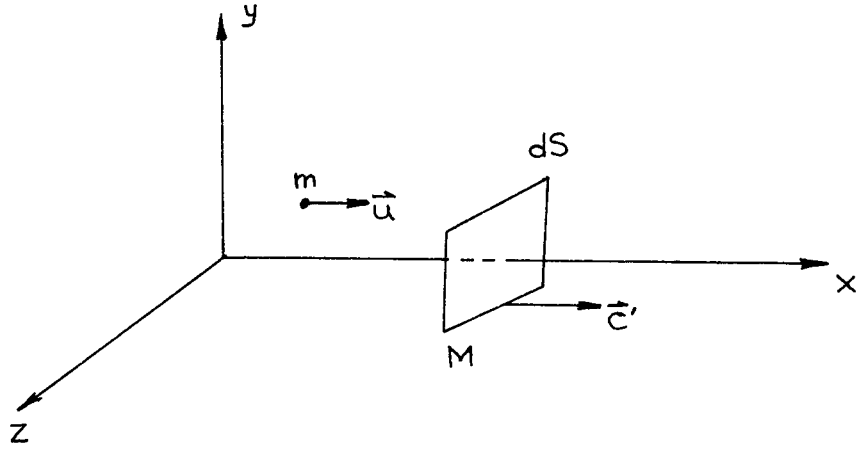

Figure A-3

at $\vec{c}$ within $d\vec{c}$ and at time t to be

$$f(\vec{r}, \vec{c}, t)\, d\vec{r}\, d\vec{c}$$

where $f(\vec{r}, \vec{c}, t)$ is the Maxwellian velocity distribution function. This function is

Eq. 1 $$f(\vec{r}, \vec{c}, t) = n(\pi^{1/2} c_o)^{-3} \exp\left[-\frac{(u^2 + v^2 + w^2)}{c_o^2}\right]$$

where n is the concentration of gas molecules and c_o is the mean molecular speed. In terms of the temperature T, Boltzmann constant k, and molecular mass m,

Eq. 2 $$c_o = \left(\frac{2kT}{m}\right)^{1/2}$$

A molecule with velocity $\vec{u}$ will strike dS in the time interval dt if it is in the volume (u-c') dS dt at time T. The average number of molecules with velocity $\vec{c}$ within $d\vec{c}$ which will strike dS in dt from the left as shown in Figure A-3 is thus

$$(u-c')f(\vec{r}, \vec{c}, t)\, dS\, d\vec{c}\, dt$$

provided dt is short enough or the gas pressure is low enough that the molecules traverse the distance (u-c') dt without colliding with other molecules. If $M >> m$ and we assume the molecules undergo elastic collisions with dS, the change in momentum ΔP of a molecule of

mass m upon striking dS from the left is

$$\Delta P = 2m(u-c')$$

The total momentum transferred to dS from the left in dt is the change in momentum ΔP_L of the molecules striking dS from the left in dt

Eq. 3 $$\Delta P_L = dS\, dt \int_{-\infty}^{\infty}\int_{-\infty}^{\infty}\int_{c'}^{\infty} 2m\,(u-c')^2\, f(\vec{r},\ \vec{c},\ t)\, du\, dv\, dw$$

Similarly, the total momentum transferred to dS from the right in dt is

Eq. 4 $$\Delta P_R = dS\, dt \int_{-\infty}^{\infty}\int_{-\infty}^{\infty}\int_{-c'}^{\infty} 2m\,(u+c')^2\, f(\vec{r},\ \vec{c},\ t)\, du\, dv\, dw$$

The net momentum change of dS in dt due to the presence of gas is thus

Eq. 5 $$\Delta P_{net} = 2m\, dS\, dt \int_{-\infty}^{\infty}\int_{-\infty}^{\infty}\left[\int_{-c'}^{\infty}(u+c')^2 f\, du - \int_{c'}^{\infty}(u-c')^2 f\, du\right] dv\, dw$$

Using the relationship

$$\int_{-\infty}^{\infty} e^{-a^2x^2}\, dx = \frac{\sqrt{\pi}}{a}$$

substituting for f from equation 1 and integrating over v and w, we obtain

Eq. 6 $$\Delta P_{net} = \frac{2mn\, dS\, dt}{c_o\sqrt{\pi}}\left[\int_{-c'}^{\infty}(u+c')^2 \exp\left[\frac{-u^2}{c_o^2}\right] du - \int_{c'}^{\infty}(u-c')^2 \exp\left[\frac{-u^2}{c_o^2}\right] du\right]$$

Let the bracketed terms in equation 6 be indicated by:

Eq. 7 $$I = \int_{-c'}^{\infty} (u+c')^2 \exp\left[\frac{-u^2}{c_o^2}\right] du - \int_{c'}^{\infty} (u-c')^2 \exp\left[\frac{-u^2}{c_o^2}\right] du$$

$$= I_1 + I_2$$

$$I_1 = \int_{-c'}^{\infty} (u+c')^2 \exp\left[\frac{-u^2}{c_o^2}\right] du$$

$$I_1 = \int_{0}^{\infty} (u+c')^2 \exp\left[\frac{-u^2}{c_o^2}\right] du + \int_{-c'}^{0} (u+c')^2 \exp\left[\frac{-u^2}{c_o^2}\right] du$$

Eq. 8 $$I_1 = \int_{0}^{\infty} (u+c')^2 \exp\left[\frac{-u^2}{c_o^2}\right] du + \int_{0}^{c'} (u-c')^2 \exp\left[\frac{-u^2}{c_o^2}\right] du$$

In the second term on the right hand side of equation 8 we have changed the variable of integration from u to -u and interchanged the limits of integration. Similarly, we find

$$-I_2 = \int_{c'}^{\infty} (u-c')^2 \exp\left[\frac{-u^2}{c^2}\right] du,$$

Eq. 9 $$-I_2 = \int_{0}^{\infty} (u-c')^2 \exp\left[\frac{-u^2}{c_o^2}\right] du - \int_{0}^{c'} (u-c')^2 \exp\left[\frac{-u^2}{c_o^2}\right] du$$

Summing the results of equation 8 and 9

Eq. 10 $$I = I_1 + I_2 = \int_{0}^{\infty} 4uc' \exp\left[\frac{-u^2}{c_o^2}\right] du + \int_{0}^{c'} 2(u-c')^2 \exp\left[\frac{-u^2}{c_o^2}\right] du$$

Equation 10 may be simplified by integrating the first term on the right hand side directly, and by expanding the squared factor and evaluating the second integral. The result after combining terms is:

Eq. 11 $$I = c_o^2 \left\{ c' \exp\left[-\left(\frac{c'}{c_o}\right)^2\right] + \left[1 + 2\left(\frac{c'}{c_o}\right)^2\right] \int_0^{c'} \exp\left[\frac{-u^2}{c_o^2}\right] du \right\}$$

and the net change in momentum of dS is

Eq. 12 $$\Delta P_{net} = \frac{dS\ dt(2mn\, c_o)}{\sqrt{\pi}} \left\{ c' \exp\left[-\left(\frac{c'}{c_o}\right)^2\right] + \left[1 + 2\left(\frac{c'}{c_o}\right)^2\right] \int_0^{c'} \exp\left[\frac{-u^2}{c_o^2}\right] du \right\}$$

The work dE performed by a force on a body in moving the body a distance dx is

Eq. 13 $$dE = F\, dx.$$

We know from the statement of Newton's second law that

$$F = \frac{dP}{dt}.$$

Substituting this result into equation 13 we find

Eq. 14 $$dE = \left(\frac{dx}{dt}\right) dP = c'\, dP$$

The work done by the gas on the element of the reed dS in dt is thus

Eq. 15 $$dE = dS\,dt\left(\frac{2mn\,c_o c'}{\sqrt{\pi}}\right)\left\{c' \exp\left[-\left(\frac{c'}{c_o}\right)^2\right] + c_o\left[1 + 2\left(\frac{c'}{c_o}\right)^2\right]\int_0^{c'/c_o} \exp\left[-x^2\right]dx\right\}$$

Since $\left(\frac{c'}{c_o}\right) << 1$ for cases of interest, the exponential terms in equation 15 may be expanded without large error and terms of $\left(\frac{c'}{c_o}\right)^2$ and larger ignored. The result is

Eq. 16 $$dE = dS\,dt\left[\frac{4mn\,c_o (c')^2}{\sqrt{\pi}}\right] \text{ for } \left(\frac{c'}{c_o}\right) << 1.$$

The value of "internal friction" due to the presence of gas may now be determined from

Eq. 17 $$Q^{-1} = \frac{\Delta E}{2\pi E}.$$

If $c'(y, t) = c'_m(y) \sin \omega t$ is the velocity of the reed in the x direction at point y along the length of the reed at time t, then the energy lost by the reed in one cycle is

$$\Delta E = \int_0^L 4b \int_0^{\tau/4} \frac{4mn\,c_o}{\sqrt{\pi}} \left[c'(y, t)\right]^2 dy\,dt$$

Eq. 18 $$\Delta E = \frac{2bmn\,c_o \tau}{\sqrt{\pi}} \int_0^L \left[c'_m(y)\right]^2 dy.$$

In equation 18, τ denotes the period of oscillation, b the width and L the length of the reed, Similarly, the energy stored in the reed is

Eq. 19 $$E = \frac{1}{2}\int_0^L \left[c'_m(y)\right]^2 dM = \frac{1}{2}\rho b a \int_0^L \left[c'_m(y)\right]^2 dy$$

where ρ is the density of the reed material and a is the thickness of the reed. Substituting from equations 18 and 19 into equation 17, and using $\nu = \frac{1}{\tau}$ as the frequency of oscillation,

Eq. 20 $$Q^{-1} = \frac{2mn\, c_o \tau}{\pi^{3/2} \rho a} = \frac{2mn\, c_o}{\pi^{3/2} \rho \nu a}$$

Eq. 21 $$Q^{-1} = \frac{2}{\pi}\left(\frac{2m}{\pi k T}\right)^{1/2} \frac{p}{\rho \nu a}$$

For air, with pressure expressed in dynes/cm^2,

$$Q^{-1} = (3.0 \times 10^{-3}) \frac{p}{\rho \nu a\, T^{1/2}} .$$

For the conditions of this experiment, $T \approx 300^0$K, $p \approx 30$ " Hg $\approx 40 \frac{\text{dynes}}{\text{cm}^2}$,

$$\underline{Q^{-1} = 1.56 \times 10^{-4}}$$

TABLE 2

DATA OF THIS INVESTIGATION

Explanation of the symbols used in this table:

V - voltage applied to the transducer, rms volts

T* - measured temperature of the reed, Celcius degrees The asterisk indicates that in runs 10-42 the temperature is the uncorrected thermometer reading.

P - pressure in vacuum enclosure, microns of mercury

$\bar{y}$ - average amplitude of vibration at resonance, units are .0793 millimeters

Q^{-1} - internal friction

The data in this table refers to reed #4 with a free length of 2-3/8 inches.

TABLE 2. (CONT.) - DATA OF THIS INVESTIGATION

Run	V (rms volts)	T* (°C)	P (μ Hg)	$\bar{y}$ (.0793 mm)	$\Omega^{-1} \times 10^4$
1-9	Preliminary Testing				
10	1.0	28	41	1.960	2.95
11	2.0	29	40	3.571	3.14
12	2.0	28	36	3.742	3.14
13	1.0	28	35	2.004	2.97
14	3.0	28	35	5.436	2.96
15	4.0	28	34	7.050	2.95
16	1.0	48	44	1.732	3.12
17	2.0	47	46	3.273	3.52
18	3.0	48	42	4.851	3.50
19	4.0	48	41	6.739	3.19
20	1.0	71	43	1.965	3.02
21	2.0	71	43	3.768	2.96
22	3.0	71	43	5.470	2.96
23	4.0	71	42	7.137	2.99
24	---	--	--	-----	----
25	1.0	88	49	1.878	3.33
26	2.0	89	49	3.633	3.17
27	3.0	90	49	5.258	3.17
28	4.0	90	49	6.703	3.14
29	1.0	106	47	1.939	----
30	2.0	105	47	3.591	3.36
31	1.0	105	46	1.904	3.20
32	3.0	105	46	5.248	3.36
33	4.0	105	45	6.866	3.13
34	1.0	137	63	1.738	3.34
35	2.0	137	62	3.344	3.34
36	3.0	137	62	4.878	3.34
37	4.0	138	58	6.449	3.34
38	1.0	170	60	1.745	3.48
39	2.0	171	60	3.370	3.32
40	3.0	171	60	4.839	3.32
41	4.0	171	59	6.311	3.48

TABLE 2. (CONT.) - DATA OF THIS INVESTIGATION

Run	V (rms volts)	T* (°C)	P (μ Hg)	$\bar{y}$ (.0793 mm)	$Q^{-1} \times 10^4$
42	2.0	189	61	3.232	3.51
43	2.0	29	50	3.934	3.22
44	1.0	30	49	2.109	3.22
45	3.0	29	48	5.694	3.22
46	4.0	29	47	7.337	3.38
47	1.0	41	41	2.194	3.04
48	2.0	41	40	4.119	3.22
49	3.0	41	40	5.890	3.22
50	4.0	41	39	7.437	3.22
51	1.0	60	33	2.229	2.71
52	2.0	60	33	4.282	2.71
53	3.0	60	31	6.175	2.71
54	2.0	25	27	4.265	3.05
55	1.0	49	28	2.227	2.71
56	2.0	50	28	3.991	3.05
57	3.0	50	28	5.503	3.22
58	1.0	68	28	2.244	2.71
59	2.0	68	29	4.184	2.71
60	3.0	67	29	5.996	2.71
61	1.0	87	28	1.914	2.88
62	2.0	88	29	3.612	2.88
63	3.0	89	29	5.140	3.05
64	1.0	101	27	2.029	2.71
65	2.0	101	28	3.921	2.54
66	3.0	101	28	5.655	2.54
67	1.0	113	29	1.989	2.54
68	2.0	113	29	3.857	2.54
69	3.0	111	28	5.703	2.54

TABLE 2. (CONT.) - DATA OF THIS INVESTIGATION

Run	V (rms volts)	T* (^{o}C)	P (μ Hg)	$\bar{y}$ (.0793 mm)	$\Omega^{-1} \times 10^{4}$
70	1.0	123	27	1.961	2.71
71	2.0	123	28	3.791	2.71
72	3.0	124	28	5.463	2.71
73	1.0	133	28	2.003	2.54
74	2.0	133	28	3.836	2.54
75	3.0	133	28	5.357	2.54

TABLE 3

SAMPLE DATA SHEET

Run No._____ Date_____

Initial Conditions:

Time start_____ Transducer voltage_____ Temperature____

Pressure_____ Freq. Red. Factor_____ Thermocouple EMF #1_____ #2_____

Resonant Frequency Determination:

Frequency Meter Dial Reading	Filar Eyepiece Setting	Rest Position Reading of Filar Eyepiece
_____	_____	_____
_____	_____	_____ Initial
_____	_____	_____
Total _____	Total _____	_____
Ave. _____	Ave._____	_____ Final
f_o _____	Amplitude_____	Ave._____

Half-power Frequency Determination:

Half-power amplitude_____

Frequency Meter Dial Reading/half-power pt. #1	Frequency Meter Dial Reading/half-power pt. #2
_____	_____
_____	_____
_____	_____
Total _____	Total _____
Ave. _____	Ave. _____
f_1 _____	f_2 _____

Rest Position Reading of Filar Eyepiece	Final Conditions:
_____	Pressure_____ Temperature_____
_____	Time Finish_____ Thermocouple EMF #1_____
_____	#2_____
_____	Internal Friction_____
Ave. _____	Strain Amplitude_____

Remarks: